

FOURTEENTH CONFERENCE ON APPLIED CLIMATOLOGY

J1.2 IRRIGATION-INDUCED WARMING IN CENTRAL CALIFORNIA?

John R. Christy and William B. Norris
University of Alabama in Huntsville, Huntsville, Alabama USA

1. INTRODUCTION

Why do temperatures rise at some stations over decades and not at others nearby? What locally varying forcing could be responsible? A general increase in temperature of some stations in Central California provides an opportunity to examine possible causes since there is a means to factor out specific influences for specific stations. However, considerable, manual work is required to extract information that allows the heterogeneous surface data to be homogenized for the detection of trends which may be used to understand causes.

2. DATA AND METHOD

We examined over 35 stations in Central California bounded between $+35.75^\circ$ and $+37.25^\circ$ latitude and -118.5° and -121° longitude (Fig 1). These stations encompass the foothills of the Coast Range on the west and the Sierra Nevada mountains on the east. Running roughly NW-SE between these two elevated features is the flat basin of the San Joaquin Valley. We divide the stations into three levels, valley ($<200\text{m}$), foothills ($200\text{-}1000\text{m}$) and mountain ($>1000\text{m}$). The valley stations are virtually all surrounded by irrigated farmland, a characteristic which separates them from the more elevated stations.

The daily Tmax and Tmin temperatures were obtained from several sources, mainly the newly digitized COOP data released by NCDC. However, these data records have significant discontinuities which must be assessed before utilizing the technique of homogeneous segment construction described in Christy (2002).

In this technique, breakpoints are identified from information contained in the meta-data files of the individual station records. These metadata forms are now archived in digital image format. We obtained all of the pertinent images which in

one way or another described the status of our stations and any changes that occurred along the way. Forms such as B-23, B-44, 530, 531, 4005, 4017, 4025, 4302, and 4303 were examined. While viewing over 2000 pages we documented every station change indicated on the forms. Once the information was systematically placed and collated in a spreadsheet, we reexamined all meta-data and determined those points in time when a discontinuity occurred. This aspect of the research was especially tedious and inserted a level of subjective interpretation into the process.

Most discontinuities dealt with station moves. A break was identified when a station moved a distance of at least 3 m. Though this distance is minuscule compared to meteorological space scales, what we often found was that the new, nearby location usually differed in some other aspect besides location alone. In one case, a 7m location change took the instrument shelter out of a sprinkler's watering pattern. Other small moves changed the exposure relative to nearby buildings. Breaks were also recorded when new instrumentation was installed or a major repair of the station infrastructure was noted. In applying these tests to 14 valley stations, for example, we generated 60 individual homogeneous segments for 1930 to 2000.

Using an iterative procedure, a bias vector was calculated which linked all of the homogeneous segments into a time series. The process essentially finds the relative bias of each segment which provides a best fit so as to minimize differences in overlapping periods (Christy 2002). The underlying assumption is that for each region, the long term variations for each station are identical to all others in the region.

Below is an example of spring (MAM) Tmax biases for valley stations where: seg is segment number, Date1 and Date2 are beginning and end of segment, Mon1 is length of segment in months, Mon2 is number of data months (MAM

Corresponding Author address: John R. Christy, ESSC/NSSTC, University of Alabama in Huntsville, Huntsville AL 35899. christy@nsstc.uah.edu

only) from other stations overlapping with this segment and Bias is the computed relative bias of the segment. Segments without sufficient data are skipped.

Seg	Name	Date1	Date2	Mon1	Mon2	Bias
1	Clov	193103	194705	45	389	0.21
2	Corc	194503	195905	45	389	-0.06
3	Corc	196003	196903	28	228	0.32
4	Corc	196904	198505	50	374	1.06
5	Corc	198603	199405	27	216	0.20
6	Corc	199503	200104	20	158	0.31
10	Five	194903	195405	18	156	0.40
11	Five	195504	195705	6	50	1.38
12	Five	195803	198405	32	268	0.51
13	Five	198503	199304	20	167	-0.35
14	Five	199505	200004	13	104	-0.49
15	Five	200012	200104	2	16	0.35
16	Fres	199903	200104	8	65	-0.25
17	Fres	193103	193305	9	63	-0.60
18	Fres	193403	194905	48	425	-0.40
19	Fres	195003	196005	33	282	-0.97
20	Fres	196103	199505	105	813	0.00
21	Fres	199603	200104	17	136	-0.82
22	Hanf	193103	193705	21	163	0.21
23	Hanf	193803	195403	47	421	-0.63
24	Hanf	195404	195505	5	44	-0.03
25	Hanf	195603	196505	26	219	0.85
26	Hanf	196603	197505	28	212	0.50
27	Hanf	197603	197905	11	83	-0.25
28	Hanf	198003	198405	15	113	-0.18
29	Hanf	198503	200104	50	398	-0.63
30	Helm	193103	194304	37	313	0.82
31	Lemo	193103	193904	24	193	-0.03
32	Lemo	193905	194705	25	230	0.78
33	Lemo	194803	197203	73	600	0.30
34	Lemo	197205	197704	14	100	-0.45
35	Lemo	197705	199805	64	501	0.24
36	Lemo	199903	200104	8	65	0.13
37	Lind	193103	194605	48	412	0.95
38	Lind	194703	194805	6	50	0.02
39	Lind	194903	197305	75	611	0.42
40	Lind	197403	200104	82	641	0.93
42	Made	193503	193704	6	53	-0.73
43	Made	193705	193805	4	33	-0.63
44	Made	193903	194405	18	165	-0.04
45	Made	194503	196205	50	434	0.61
46	Made	196303	197405	32	248	-0.13
47	Made	197503	198505	25	200	-0.10
48	Made	198603	200005	42	336	-0.89
49	Oran	193203	196405	94	808	-0.30
50	Oran	196503	196505	3	26	-0.13
51	Oran	196603	199005	38	305	-0.06
52	Port	193103	193705	21	163	-0.05
53	Port	193803	193905	6	52	-0.24
54	Port	194003	194705	24	222	0.21
55	Port	194803	195405	21	179	-0.12
56	Port	195503	196303	24	200	0.53
57	Port	196304	200104	115	893	0.84
58	Visa	193903	196404	77	670	0.67
59	Visa	196405	197005	18	143	-0.39
60	Visa	197103	197105	3	21	-0.23
61	Visa	197203	198704	47	353	-0.27
62	Visa	198705	199405	22	175	-1.31
63	Visa	199503	200104	20	158	-1.11
65	West	193303	194605	37	329	-0.64

3. IRRIGATION

The Mediterranean climate of the San Joaquin Valley is characterized by a hot, dry season from May through October. Average annual precipitation totals in the valley range from 12 to 30 cm while orographically enhanced amounts in the mountains may exceed 200 cm. Usually, less than 10% falls during May to October.

Irrigated acreage in the five counties of Central California (Merced, Madera, Fresno, Kings and Tulare) has risen by a factor of 5 over the 20th century. Early systems were simply diversion canals which redistributed water to areas near the available rivers. During the 20th century, extensive, multi-year storage reservoirs along with concrete-lined canals stretching over 100 km were built to hold back spring runoff for release throughout the year for agriculture.

Today, the pre-20th century San Joaquin Valley is fondly remembered as the Serengeti of North America. An estimated 10,000 grizzly bears, hundreds of thousands of antelope and hundreds of millions of migrating water fowl lived in the valley for at least a portion of each year. Rivers flowed uninterrupted to the Delta region and supported significant salmon runs. With the stoppage of the rivers and their diversion to irrigated land (an average acre requires over 1m of water per year) the ecosystem changed dramatically. Without irrigation, the valley environment would be characterized as very dry and desert-like from late spring to late fall every year. With very low humidity, such an environment saw diurnal temperature ranges of over 15°C in the dry season. Additionally, the hard, dry natural surface had little heat capacity and relatively high albedo.

4. RESULTS

We calculated trends for each season and elevation layer for the 1930-2000 period. The most remarkable difference in trends among the valley, foothill and mountain stations is found in summer (JJA). Tmin and Tmax time series are shown in Figs. 2a and 2b. Note that the mountain trends (green) for both Tmax and Tmin are near zero. Tmax trends for valley (red) and foothill (blue) stations are slightly negative. However, the Tmin trend is significantly positive while that of the nearby foothill stations is near zero.

A complete picture for all seasons is shown in Fig. 3. Most prominent are the Tmin trends for

the valley stations, all being significantly positive. However, for the nearby foothill stations, T_{min} trends are rather unremarkable. In their difference, one sees a distinct annual cycle which correlates well with the irrigation deliveries for the valley farms.

T_{max} trends are revealing in a different way. For both valley and foothill, the sign, ranking and magnitude of the two elevations are statistically indistinguishable. This gives confidence that these independent sets of stations are providing realistic results.

Our hypothesis at this point is that irrigation has altered the surface energy balance of the valley floor, causing nighttime temperatures to remain warm. There are three possibilities related to irrigation. First, the additional water vapor supplied through evaporation, not present formerly, enhances the downward flux of thermal radiation. Second, the additional vapor allows aerosols to reach the swelling point at which they become very active in the thermal spectrum. Last, the moist ground and vegetation absorb solar energy during the ubiquitous cloudless days, and release the energy in the evening.

At this point our view is that the last process is the dominant one. Preliminary calculations indicate the enhanced water-vapor greenhouse effect would be relatively small while the humidity does not usually exceed the 80% threshold to initiate aerosol swelling. Thus, the presence of liquid water in the ground and

vegetation (with lower albedo) increases the thermal capacity of the surface, thus keeping the nighttime temperatures warmer than would be otherwise through sensible heat flux.

During the day, however, it is likely that enhanced evaporation would induce lower values of T_{max}. This is consistent with the declining trend in JJA for the valley. During the day also, the atmospheric boundary layer deepens and thus the evaporational cooling has opportunity to spread its influence through the deeper layer, possibly encompassing the foothill stations. Note that both valley and foothill T_{max} trends are negative.

Our next step is to test our hypothesis with a high resolution, mesoscale model with significant boundary layer physics to determine if our conjectures are supported.

In the broader sense, one should note that the annual trends of the valley and foothills (Fig 3) are quite different. We hypothesize that this difference is due to irrigation. It is also obvious that whatever the forcing is that contributes to these trends is likely not global in nature, such as forcing from carbon dioxide. Such a forcing should be apparent at all elevations.

5. REFERENCES

- Christy, J.R., 2002: When was the hottest summer? A State Climatologist struggles for an answer. Bull. Am. Meteor. Soc., 83, 723-734.

Central California

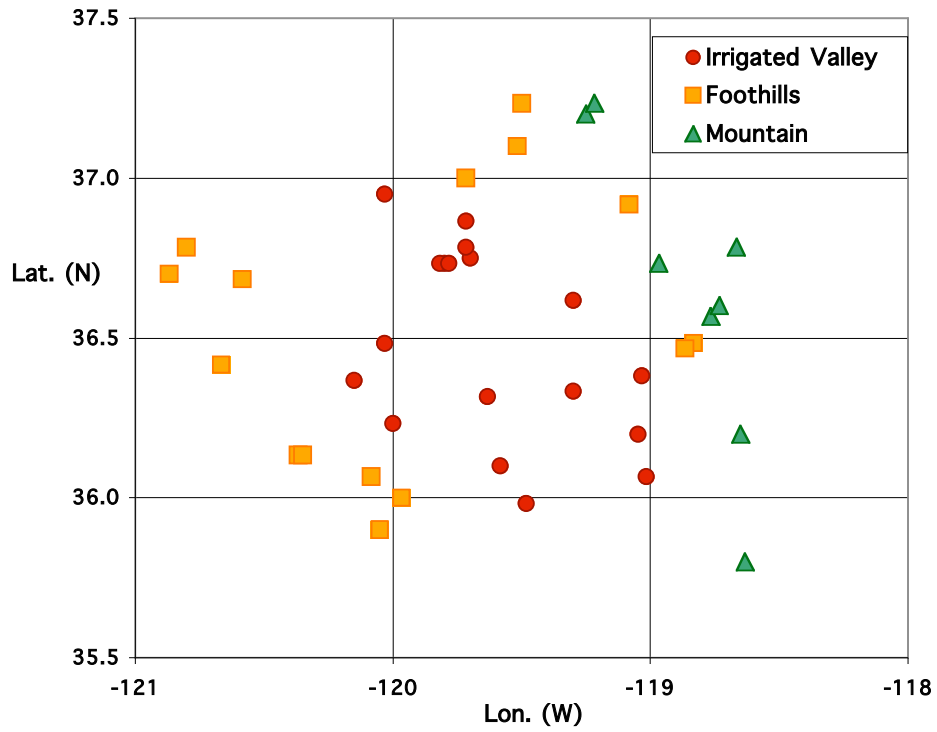
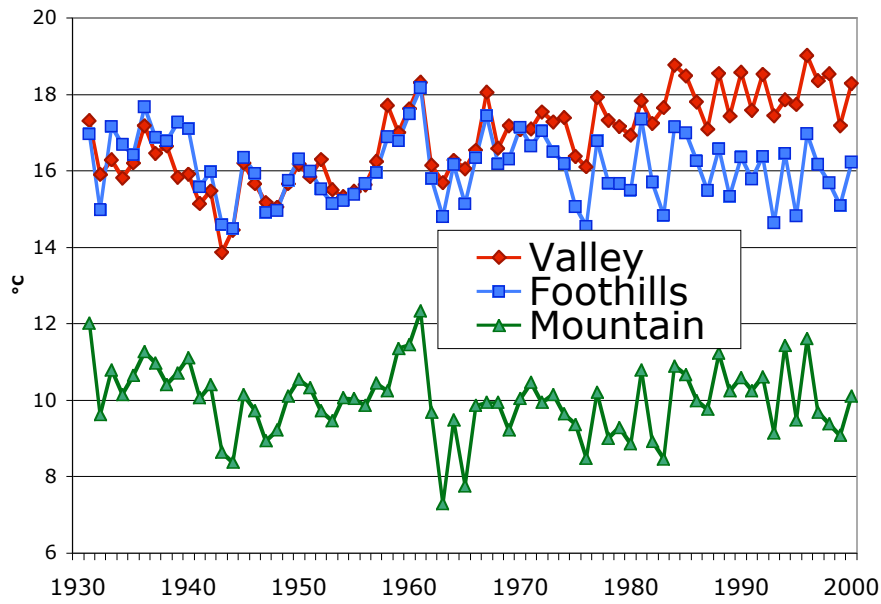


Fig. 1. Location of stations used in this study. Elevation levels: valley <200m, foothill, 200 to 1000m, mountain >1000m. A single station may be represented by more than one indicator on the map due to location changes.

TMin Central California JJA



TMax Central California JJA

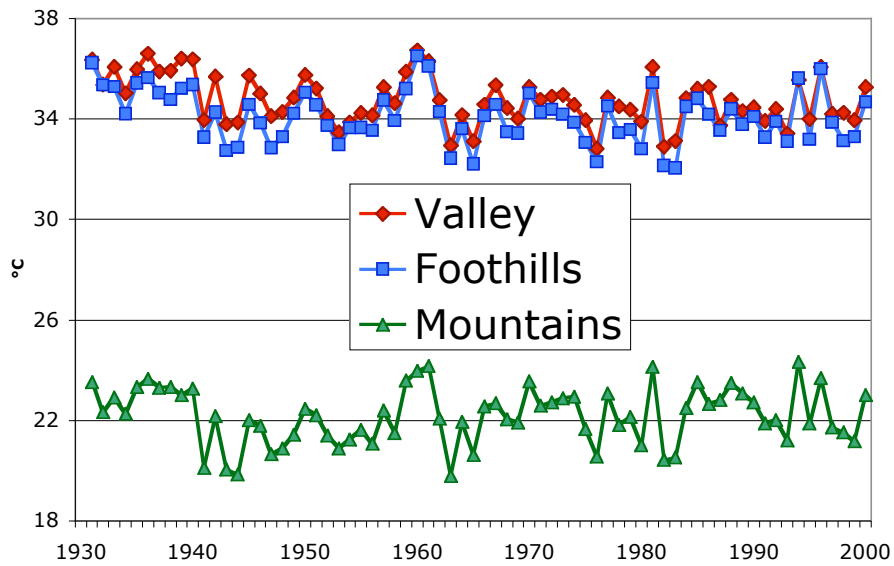


Fig 2a (top) time series of seasonal daily minimum temperature anomalies for 1930-2000. 2b, as in 2a for daily maximum temperature anomalies.

**Valley and Foothill Temperature Trends 1931-2000
Central California (Preliminary)**

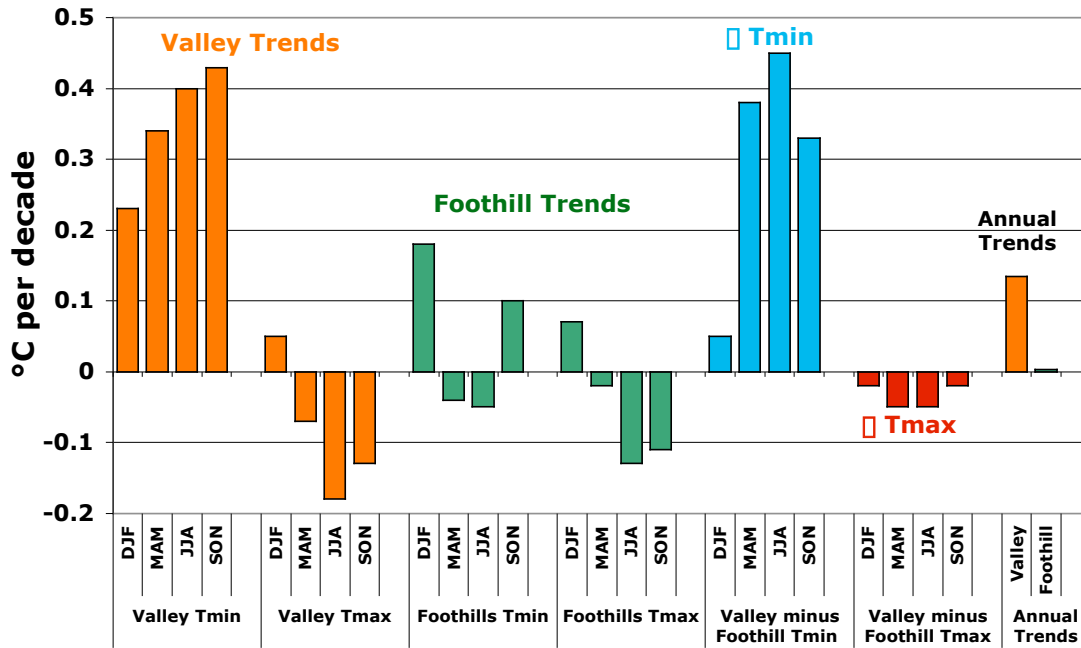


Fig. 3. Bar chart of seasonal temperature trends of daily maximum and minimum temperatures for valley (orange) and foothill (green) stations. Differences in seasonal trends are shown in blue (Tmin) and red (Tmax). Annual trends are shown at the far right.